Critical properties of the 3D-Heisenberg ferromagnet $CdCr_2Se_4$

A Letters Journal Exploring the Frontiers of Physics

September 2010

EPL, **91** (2010) 57001
doi: 10.1209/0295-5075/91/57001

www.epljournal.org

Critical properties of the 3D-Heisenberg ferromagnet $CdCr_2Se_4$

Lei Zhang[1(a)], Jiyu Fan[2], Li Li[3], Renwen Li[1,4], Langsheng Ling[1], Zhe Qu[1], Wei Tong[1], Shun Tan[3] and Yuheng Zhang[1,3]

[1] *High Magnetic Field Laboratory, Chinese Academy of Sciences - Hefei 230031, PRC*
[2] *College of Science, Nanjing University of Aeronautics and Astronautics - Nanjing 210016, PRC*
[3] *Hefei National Laboratory for Physical Sciences at the Microscale, University of Science and Technology of China Hefei 230026, PRC*
[4] *Department of Physics and Electronic Engineering, Hefei Normal University - Hefei 230061, PRC*

received on 15 August 2010; accepted by J. F. Scott on 18 August 2010
published online 3 September 2010

PACS 76.50.+g – Ferromagnetic, antiferromagnetic, and ferrimagnetic resonances; spin-wave resonance
PACS 75.40.-s – Critical-point effects, specific heats, short-range order
PACS 76.30.-v – Electron paramagnetic resonance and relaxation

Abstract – The critical properties of the ferromagnet $CdCr_2Se_4$ around the paramagnetic-ferromagnetic phase transition have been investigated. It is found that the 3D-Heisenberg model is the best one to describe the critical phenomena around the critical point. Critical exponents $\beta = 0.337 \pm 0.03$ and $\gamma = 1.296 \pm 0.109$ at $T_C = 130.48 \pm 0.34$ are obtained. In addition, the critical exponent $\delta = 4.761 \pm 0.129$ is determined separately from the isothermal magnetization at T_C. These critical exponents fulfill the Widom scaling relation $\delta = 1 + \gamma/\beta$. Based on these critical exponents, the magnetization-field-temperature (M-H-T) data around T_C collapses into two curves obeying the single scaling equation $M(H, \varepsilon) = \varepsilon^{\beta} f_{\pm}(H/\varepsilon^{\beta+\gamma})$. Although the 3D-Heisenberg model is the most satisfactory model to describe this system, critical exponents for $CdCr_2Se_4$ are slightly smaller than the theoretical exponents ($\beta = 0.36$, $\gamma = 1.39$ and $\delta = 4.8$). This indicates that the exchange interaction $J(r)$ decays slower than r^{-5} in this system, which can be attributed to the spin-lattice coupling.

Introduction. – Although the selenide $CdCr_2Se_4$ has been studied intensively for many decades, it still remains in hot investigations for lots of fantastic physical characteristics related to ferromagnetic or ferroelastic order and electronic transport properties [1–7]. This spinel structural compound belongs to the cubic cell structure with space group $Fd\bar{3}m$ [8]. The Cr ions occupy the octahedral sites in the spinel B sublattice, and Cd occupies the tetrahedrally coordinated A sublattice. Its valence configuration is $Cd^{2+}Cr_2^{3+}Se_4^{2-}$ with only Cr^{3+} ($3d^3$) possessing the magnetic moments $\boldsymbol{S} = 3/2$ [7,8]. It is an n-type semiconductor in transport properties, which can be changed into a p-type one by selenium vacancies [9].

The magnetic properties of $CdCr_2Se_4$ have attracted much considerable attention. The magnetization experiences an abrupt paramagnetic-ferromagnetic (PM-FM) phase transition at $T_C \sim 130\,\mathrm{K}$ upon cooling. The large paramagnetic Curie-Weiss temperature T_{CW} indicates strong ferromagnetic exchange interactions. In the ferromagneitc ordered phase, the saturation magnetization was reported to be in the range of 5.4–5.98 μ_B/mol, which is close to the value expected for the magnetic moments carried by Cr^{3+} ions [1,7,10,11]. In fact, the magnetic ordered state in the spinel AB_2X_4 is determined by the competition between the nearest-neighbor ferromagneitc superexchange B-X-B and high-order-neighbor antiferromagnetic B-X-A-B-X interactions, while the ferromagnetic superexchange is dominant in the $CdCr_2Se_4$ system [5]. As a result, the mechanism of the magnetic phase transition of this system is considered as the 90° Cr^{3+}-Se^{2-}-Cr^{3+} superexchange, which is in accordance with the Kanamori-Goodenough rules [12,13].

On the other hand, $CdCr_2Se_4$ is very close to the ideal isotopic Heisenberg ferromagnet required to test various theories of the critical phenomena in magnetic materials [7]. To better understand the Heisenberg ferromagnetism and the basic physical mechanisms, it is important to fully understand the PM-FM transition at

(a) E-mail: zhanglei@hmfl.ac.cn

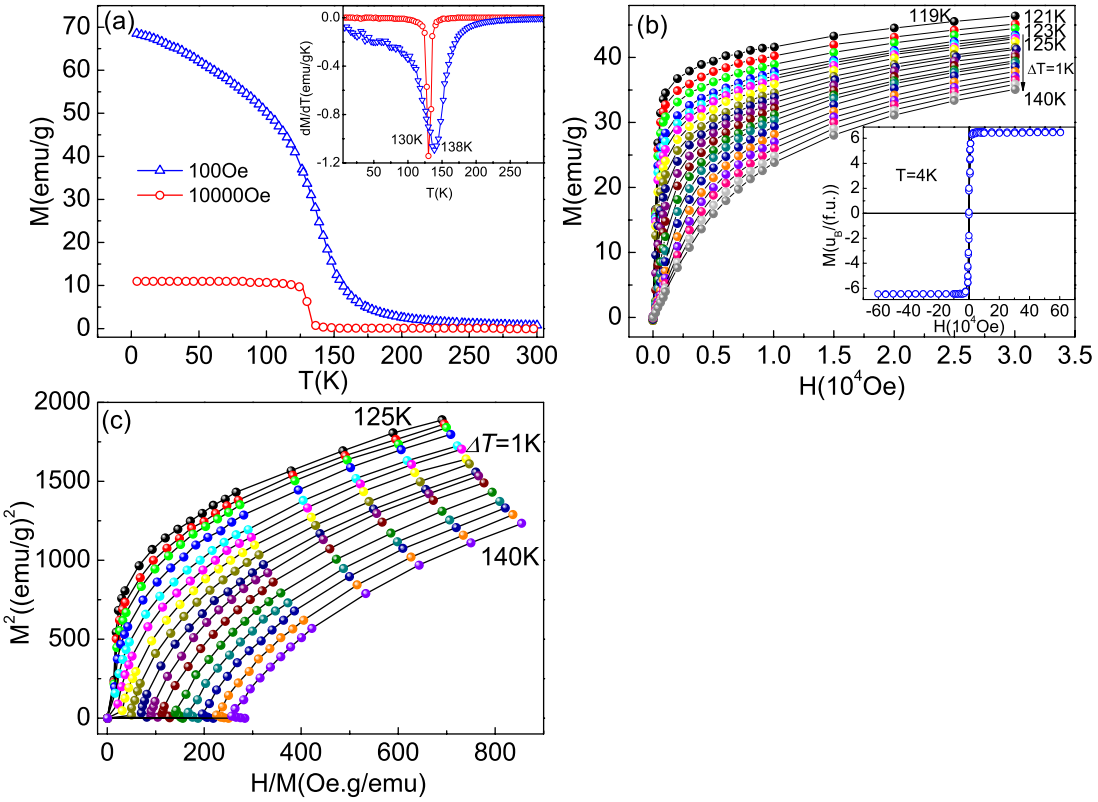

Fig. 1: (Color online) (a) The temperature dependence of magnetization under $H = 100$ Oe and 10000 Oe (the inset plots dM/dT *vs.* T); (b) the isothermal magnetization around T_C for $CdCr_2Se_4$ (the inset is the isothermal magnetization at 4 K); (c) Arrott plot: Isotherms of M^2 *vs.* H/M at temperatures around T_C for $CdCr_2Se_4$.

the critical point. Therefore, a detailed study of the critical exponents associated with the FM transition is necessary. In this work, four kinds of different theoretical models, the mean-field ($\beta = 0.5$), the 3D-Heisenberg ($\beta = 0.365$), the 3D-Ising ($\beta = 0.325$) and the tricritical mean-field ($\beta = 0.25$) model, were tried to explain the critical properties in view of the varying critical exponent β from 0.1 to 0.5 [14,15]. It is found that the selenide $CdCr_2Se_4$ is in best accordance with the 3D-Heisenberg model. Furthermore, reliable critical exponents β, γ and δ were obtained. These exponents are slightly smaller than the theoretical values, which can be explained by the decay distance of the exchange interaction.

Experiment. – A polycrystaline sample of $CdCr_2Se_4$ was prepared by the solid-state reaction method. High-purity powders of cadmium, chromium, selenium were mixed according to the stoichiometric ratio, and sealed into an evacuated quartz tube and slowly heated to 850 °C. Then the powder was pressed into pellets after sintering at 850 °C for 7 days. Finally, the pellets were sealed into an evacuated quartz tube and sintered at 850 °C for another 2 days. The powder X-ray diffraction (XRD) proved that the sample is single phase. The magnetic properties were measured using a commercial SQUID magnetometer (Quantum Design MPMS). The sample was processed to sphere shape to decrease the demagnetizating field. The electronic paramagnetic resonance (EPR) measurement of the powder sample was performed using a Bruker EMX plus model spectrometer operating at the X-band frequencies (9.4 GHz) at selected temperatures.

Results and discussion. – The temperature dependence of magnetization for $CdCr_2Se_4$ under a magnetic field of 100 Oe and 10000 Oe is shown in fig. 1(a). An abrupt PM-FM phase transition happens at T_C. The Curie temperature T_C is defined as the temperature corresponding to the extreme of dM/dT *vs.* T, as shown in the inset of fig. 1(a). It can be seen that $T_C = 130$ K under $H = 100$ Oe, while $T_C = 138$ K under $H = 10000$ Oe, which indicates that T_C is dependent on the external field H. In fact, T_C under zero field is close to that under low field (*i.e.*, $T_C|_{H=0} \sim 130$ K). However, accurate $T_C|_{H=0}$ values should be determined by the analysis of the critical exponents. Thus, the isothermal magnetization around T_C is measured for the analysis of the critical properties, as gives in fig. 1(b). The compound $CdCr_2Se_4$ is a soft ferromagnet with no coercivity force, as displayed in the inset of fig. 1(b). So, there is no magnetic hysteresis in the isothermal magnetization.

Generally, the critical exponents and critical temperature can be easily determined by analyzing the Arrott plot at temperatures around T_C [16,17]. As in the Landau theory of phase transition, the Gibbs free energy G can be

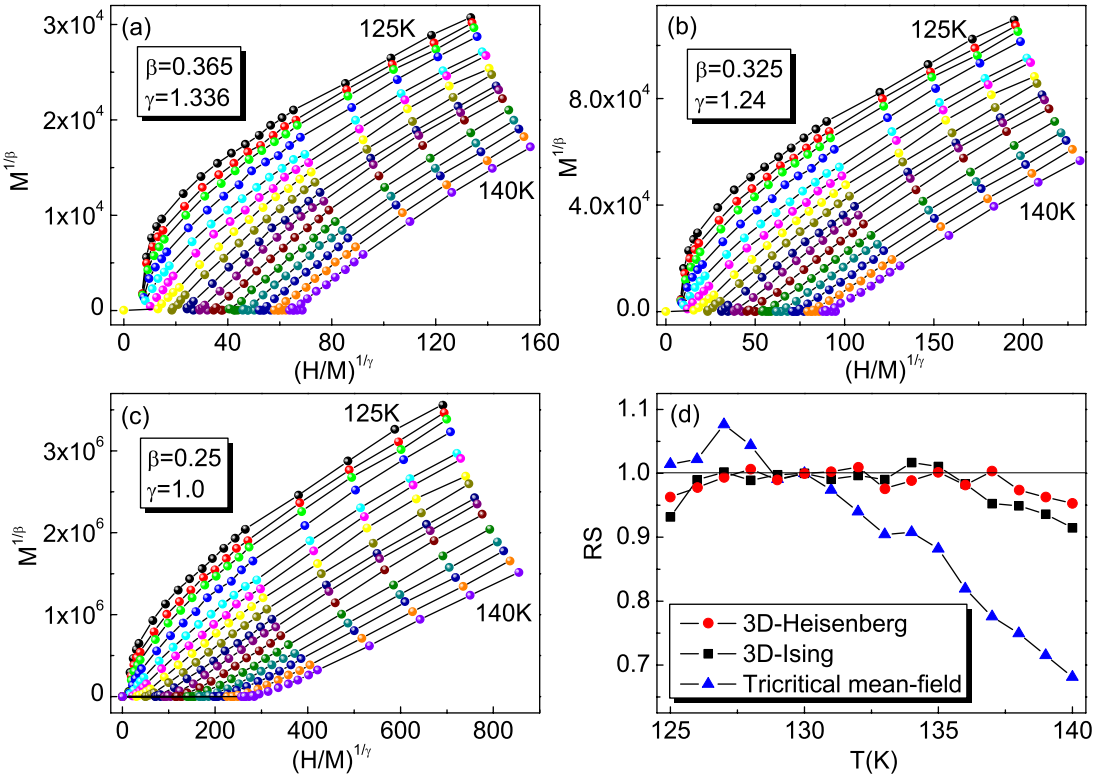

Fig. 2: (Color online) Modified Arrott plot: isotherms of $M^{1/\beta}$ *vs.* $(H/M)^{1/\gamma}$ with (a) 3D-Heisenberg model ($\beta = 0.365$, $\gamma = 1.336$), (b) 3D-Ising model ($\beta = 0.325$, $\gamma = 1.24$) and (c) tricritical mean-field model ($\beta = 0.25$, $\gamma = 1.0$); (d) relative slope (RS) as a function of temperature defined as $RS = S(T)/S(T_C = 130\,\mathrm{K})$.

expressed in terms of the order parameter M as

$$G(T, M) = G_0 + aM^2 + bM^4 - MH. \tag{1}$$

The coefficients a and b are temperature-dependent [18]. For the condition of equilibrium ($\partial G/\partial M = 0$, *i.e.*, energy minimization), the magnetic equation of state transforms to

$$H/M = 2a + 4bM^2. \tag{2}$$

Thus, the M^2 *vs.* H/M should appear as straight lines in the high-field range in the Arrott plot. The intercept of M^2 as a function of H/M on the H/M axis is negative/positive below/above T_C. The line of M^2 *vs.* H/M at T_C should cross the origin. According to the criterion proposed by Banerjee [19], the order of the magnetic transition can be determined from the slope of the straight line: the positive slope corresponding to the second-order transition while the negative slope to the first-order one. Figure 1(c) shows the Arrott plot of M^2 *vs.* H/M for $CdCr_2Se_4$ around T_C. The positive slope of the M^2 *vs.* H/M relation indicates that the PM-FM phase transition is a second-ordered one. However, all curves in the Arrott plot are nonlinear and show an upward curvature even in the high-field region, which indicates that $\beta = 0.5$ and $\gamma = 0.1$ are not satisfied according to the Arrott-Noakes equation of state $(H/M)^{1/\gamma} = (T - T_C)/T_C + (M/M_1)^{1/\beta}$ [20]. In other words, the Landau phase transition theory or the mean-field theory with $\beta = 0.5$ and $\gamma = 0.1$ is not valid for $CdCr_2Se_4$. Thus, the modified Arrott plots are employed to obtain the correct β and γ.

As is well known, the second-order magnetic phase transition can be studied in detail through a series of critical exponents. According to the scaling hypothesis, the mathematic definitions of the exponents from magnetization can be described as [21–23]

$$M_S(T) = M_0|\varepsilon|^{\beta}, \quad \varepsilon < 0, \quad T < T_C, \tag{3}$$

$$\chi_0(T)^{-1} = (h_0/M_0)\varepsilon^{\gamma}, \quad \varepsilon > 0, \quad T > T_C, \tag{4}$$

$$M = DH^{1/\delta}, \quad \varepsilon = 0, \quad T = T_C, \tag{5}$$

where ε is the reduced temperature $(T - T_C)/T_C$; M_0, h_0 and D are the critical amplitudes. β (associated with the spontaneous magnetization M_S), γ (associated with the initial magnetic susceptibility χ_0) and δ (associated with the critical isothermal magnetization at T_C) are the critical exponents.

In the high-field region, the effects of charge, lattice and orbital degrees of freedom are suppressed in a ferromagnet, and the order parameter can be identified with the macroscopic magnetization [23]. Three kinds of trial exponents of the 3D-Heisenberg model ($\beta = 0.365$, $\gamma = 1.336$), the 3D-Ising model ($\beta = 0.325$, $\gamma = 1.24$) and the tricritical mean-field model ($\beta = 0.25$, $\gamma = 1.0$) are used to make a modified Arrott plot, as shown in fig. 2(a)–(c). All the three models

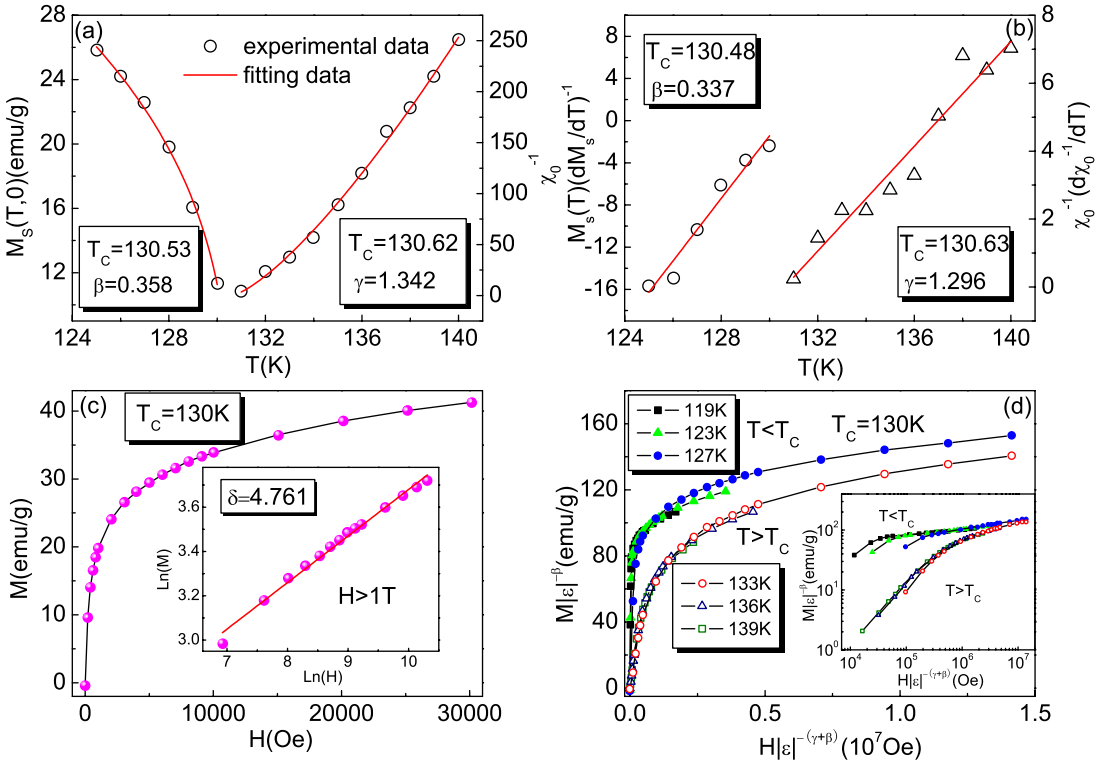

Fig. 3: (Color online) (a) The spontaneous magnetization $M_S(T,0)$ (left, open circles) and the inverse initial susceptibility $\chi_0^{-1}(T)$ (right, open circles) as a function of temperature along with the fitting curves based on the power laws (solid curves). (b) Kouvel-Fisher plot for the spontaneous magnetization $M_S(T)$ (left) and the inverse initial susceptibility $\chi_0^{-1}(T)$ (solid lines are fitted). (c) Isothermal M *vs.* H plot for $CdCr_2Se_4$ at $T_C = 130\,\mathrm{K}$ (the inset shows the same plot in log-log scale and the solid line is the linear fit following eq. (3)). (d) Scaling plot below and above T_C using β and γ determined from the Kouvel-Fisher method (only several typical curves are shown).

yield quasistraight lines in the high-field region. However, the tricritical mean-field model should be excluded firstly because these straight lines are not parallel to each other. It is difficult to determine which one is better between the 3D-Heisenberg and the 3D-Ising model from fig. 2(a) and fig. 2(b). Thus, the relative slope (RS) is defined as $RS = S(T)/S(T_C = 130\,\mathrm{K})$ in order to distinguish which model is better to describe this system. The RS of the most satisfactory model should be the one close to 1 mostly for the reason that the modified Arrott plots are a series of parallel lines [23]. The RS *vs.* T for the three models are shown in fig. 2(d), which displays that the 3D-Heisenberg model is the best one for $CdCr_2Se_4$. Therefore, the linear extrapolation from the high-field region to the intercepts with the axes $H/M^{1/\gamma}$ and $M^{1/\beta}$ yields the reliable values of the inverse initial susceptibility $\chi_0^{-1}(T,0)$ and of the spontaneous magnetization $M_S(T,0)$ respectively, which are plotted as a function of temperature in fig. 3(a) as open circles. The experimental data can be fitted according to eq. (1) and eq. (2), which gives the new critical exponents $\beta = 0.358 \pm 0.039$ with $T_C = 130.53 \pm 0.28$ and $\gamma = 1.342 \pm 0.158$ with $T_C = 130.62 \pm 0.65$, respectively. The accurate transition temperature $T_C|_{H=0} \approx 130\,\mathrm{K}$ is obtained, which is consistent with the speculation above.

On the other hand, these critical exponents can be also determined more accurately according to the Kouvel-Fisher (KF) method [24]:

$$\frac{M_S(T)}{\mathrm{d}M_S(T)/\mathrm{d}T} = \frac{T - T_C}{\beta}, \tag{6}$$

$$\frac{\chi_0^{-1}(T)}{\mathrm{d}\chi_0^{-1}(T)/\mathrm{d}T} = \frac{T - T_C}{\gamma}. \tag{7}$$

According to eq. (6) and eq. (7), $M_S(T)/\mathrm{d}M_S(T)/\mathrm{d}T$ and $\chi_0^{-1}(T)/\mathrm{d}\chi_0^{-1}(T)/\mathrm{d}T$ are plotted as linear functions of temperature, and their slopes are $1/\beta$ and $1/\gamma$, respectively. $M_S(T)/[\mathrm{d}M_S(T)/\mathrm{d}T]$ and $\chi_0^{-1}(T)/[\mathrm{d}\chi_0^{-1}(T)/\mathrm{d}T]$ *vs.* T are plotted in fig. 3(b). The new exponents are obtained as $\beta = 0.337 \pm 0.033$ with $T_C = 130.48 \pm 0.34$ and $\gamma = 1.296 \pm 0.109$ with $T_C = 130.63 \pm 0.48$, which agrees well with the theoretical prediction $\gamma = 1.2$–1.3 [25]. These exponents obtained from the KF method are inconsistent with that obtained from the modified Arrott plot of the 3D-Heisenberg model.

The third critical exponent δ can be determined according to eq. (3). As discussed above, the critical point

$T_C \sim 130$ K. The isothermal magnetization at $T_C = 130$ K is given in fig. 3(c), and the inset of fig. 3(c) plots the log-log scale. The $\ln(M) - \ln(H)$ relation yields a straight line in the higher-field range ($H > 1$ T), and the slope is $1/\delta$. Then, the third exponent $\delta = 4.761 \pm 0.129$ is obtained. According to the statistical theory, these three critical exponents obey the Widom scaling relation [26]:

$$\delta = 1 + \frac{\gamma}{\beta}. \tag{8}$$

Thus, we have $\delta = 4.749$ from fig. 3(a) and $\delta = 4.846$ from fig. 3(b), both of which are close to the one obtained from the isothermal magnetization at T_C. This proves that the critical exponents obtained here are reliable.

As a further confirmation, the critical exponents at T_C are tested according to the prediction of the scaling hypothesis. In the critical region, the magnetic equation can be written as [27]

$$M(H, \varepsilon) = \varepsilon^{\beta} f_{\pm}(H/\varepsilon^{\beta+\gamma}), \tag{9}$$

where $f_{\pm}$ are regular functions with f_+ for $T > T_C$, while we have f_- for $T < T_C$. Equation (9) indicates that $M(H, \varepsilon)\varepsilon^{-\beta}$ *vs.* $H\varepsilon^{-(\beta+\gamma)}$ forms two universal curves for $T > T_C$ and $T < T_C$, respectively. Thus, the isothermal magnetization around T_C is plotted as this prediction of the scaling hypothesis in fig. 3(d). The inset of fig. 3(d) is the log-log scale. All experiment data collapse into two different curves. This proves that eq. (9) is obeyed over the entire range of the nomalized variables, which further indicates the reliability of the obtained critical exponents.

The critical exponents obtained here is mostly close to the 3D-Heisenberg model, which indicates that $CdCr_2Se_4$ is a 3D-Heisenberg ferromagnet. As for the Heisenberg model, the exchange integral is strongly dependent on the interaction distance. In fact, the $CdCr_2Se_4$ forms a ferromagnet via the 90° Cr-Se-Cr superexchange [12]. On the other hand, the universality class of the magnetic phase transition depends on the range of the exchange interaction $J(r)$ in homogeneous magnets [28–30]. The long-range attractive interactions decay as [29]

$$J(r) \sim 1/r^{-(d+\sigma)}, \tag{10}$$

where d is the spatial dimension, $\sigma > 0$. For a three-dimensional material ($d = 3$), there holds the relation $J(r) \sim r^{-(3+\sigma)}$ with $3/2 \leqslant \sigma \leqslant 2$. When $\sigma = 2$, the Heisenberg exponents ($\beta = 0.365$, $\gamma = 1.336$ and $\delta = 4.8$) are valid for the three-dimensional isotropic ferromagnet, *i.e.*, $J(r)$ decreases faster than r^{-5}. When $\sigma = 3/2$, the mean-field exponents ($\beta = 0.5$, $\gamma = 1.0$ and $\delta = 3.0$) are valid, which indicates that $J(r)$ decreases slower than $r^{-4.5}$. All exponents obtained here are slightly smaller than the theoretical values of the 3D-Heisenberg model, which confirms that $J(r)$ decays slower than r^{-5} for $CdCr_2Se_4$.

What is the reason that causes the deviation of these critical exponents? In order to further understand the interaction at the critical point, the peak-to-peak linewidth ΔH_{pp} of the ESR spectra and the inverse M^{-1} *vs.* T are shown in fig. 4. Obviously, changes happen to the ESR spectrum with temperature cooling (see the inset of fig. 4). ΔH_{pp} decreases linearly with temperature cooling above $T_{min} \sim 155$ K, while it increases rapidly with temperature cooling below T_{min}, which indicates a strong spin interaction with another environment [31]. The $M^{-1} - T$ deviates the linear relation below $T^* \sim 210$ K, while the inflexion point locates at $T_C \sim 130$ K. These results indicate the appearance of a strong spin-lattice coupling near T_C, which is confirmed by the study of the Raman spectra [32]. This spin-lattice coupling has been also reported in other similar systems [33–35]. The spin-lattice coupling starts at T^*, leading to the deviation from the linear relation of $M^{-1} - T$. With temperature cooling, the spin-lattice coupling is enhanced rapidly, causing the rapid increase of ΔH_{pp}. Finally, the long-range super-exchange ferromagnetic coupling forms at T_C. In fact, the spin-lattice is so strong in the ferromagnetic region that it causes $J(r)$ to decay slower than r^{-5}. Therefore, the exchange interaction is affected by the spin-lattice coupling, which leads to the deviation of the critical exponents.

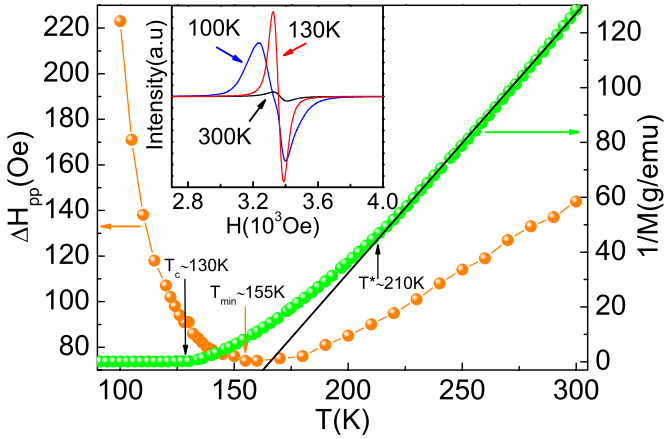

Fig. 4: (Color online) The peak-to-peak linewidth ΔH_{pp} of the ESR spectra (left axis) and the inverse M^{-1} (right axis) *vs.* T; the inset plots three typical ESR spectra at different temperatures for comparison.

Conclusion. – In conclusion, the critical phenomena of the superexchange ferromagnet $CdCr_2Se_4$ have been comprehensively studied by the isothermal dc-magnetization around the Curie point T_C. The 3D-Heisenberg model is the best to describe the critical properties. The reliable critical exponents (T_C, β, γ and δ) are obtained based on various research techniques including modified Arrott plot, Kouvel-Fisher method, and critical isotherm analysis. With these critical exponents thus obtained, the magnetization-field-temperature (M-H-T) data below and above T_C collapse into two different curves obeying the single scaling equation. Besides, these exponents indicate that the exchange

interaction $J(r)$ decays slower than r^{-5} in this system, which can be attributed to the spin-lattice coupling.

* * *

This work was supported by the State Key Project of Fundamental Research of China (2007CB925001) and the Knowledge Innovation Program of the Chinese Academy of Sciences (No. Y06CS31121BQ, Hefei institutes of Physical Science, CAS).

REFERENCES

[1] Lehmann H. W., *Phys. Rev.*, **163** (1967) 488.
[2] Miyatani K., *J. Phys. Soc. Jpn.*, **28** (1970) 259.
[3] Kanomata T., Ito H. and Kaneko T., *J. Phys. Soc. Jpn.*, **29** (1970) 332.
[4] Continenza A., Depascale T., Meloni F. and Serra M., *Phys. Rev. B*, **49** (1994) 2503.
[5] Masrour R., *J. Alloys Compd.*, **489** (2010) 441.
[6] Ohgushi K., Okimoto Y., Ogasawara T., Miyasaka S. and Tokura Y., *J. Phys. Soc. Jpn.*, **77** (2008) 034713.
[7] Baltzer P. K., Wojtowicz P. J., Robbins M. and Lopatin E., *Phys. Rev.*, **151** (1966) 367.
[8] Borovskaya T. N., Butman L. A., Tsirelson V. G., Poray-Koshits M. A., Aminov T. G. and Ozerov R. P., *Kristallografiya*, **36** (1991) 612.
[9] Kalinnikov V. T., Aminov T. G. and Novotortsev V. M., *Inorg. Mater.* (*Engl. Transl.*), **39** (2003) 997.
[10] Baltzer P. K., Lehman H. W. and Robbins M., *Phys. Rev. Lett.*, **15** (1965) 493.
[11] Lecraw R. C., Von Philipsborn H. and Sturge D., *J. Appl. Phys.*, **38** (1967) 965.
[12] Motida K. and Miyahara S., *J. Phys. Soc. Jpn.*, **29** (1970) 516.
[13] Loudghiri E., Belayachi A., Nogues M., Taibi M., Cruz M. M. and Godinho M., *J. Magn. & Magn. Mater.*, **320** (2008) 671.
[14] Kaul S. N., *J. Magn. & Magn. Mater.*, **53** (1985) 5.
[15] Huang K., *Statistical Machanics,* 2nd edition (Wiley, New York) 1987.
[16] Arrott A., *Phys. Rev.*, **108** (1957) 1394.
[17] Yeung I., Roshko R. M. and Williams G., *Phys. Rev. B*, **34** (1986) 3456.
[18] Lvy L. P., *Magnetism and Superconductivity* (Springer, Berlin) 2000.
[19] Banerjee S. K., *Phys. Lett.*, **12** (1964) 16.
[20] Arrott A. and Noakes J. E., *Phys. Rev. Lett.*, **19** (1967) 786.
[21] Fisher M. E., *Rep. Prog. Phys.*, **30** (1967) 615.
[22] Stanley H. E., *Introduction to Phase Transitions and Critical Phenomena* (Oxford University Press, London) 1971.
[23] Fan J., Ling L., Hong B., Zhang L., Pi L. and Zhang Y., *Phys. Rev. B*, **81** (2010) 144426.
[24] Kouvel J. S. and Fisher M. E., *Phys. Rev.*, **136** (1964) A1626.
[25] Freeman S. and Wojtowicz P. J., *Phys. Lett. A*, **26** (1967) 231.
[26] Kadanoff L. P., *Physics*, **2** (1966) 263.
[27] Stanley H. Eugene, *Introduction to Phase Transition and Critical Phenomena* (Oxford University Press, New York) 1971, p. 182.
[28] Ghosh K., Lobb C. J. and Greene R. L., *Phys. Rev. Lett.*, **21** (1998) 4740.
[29] Fisher M. E., Shang-Keng M. and Nickel B. G., *Phys. Rev. Lett.*, **29** (1972) 917.
[30] Zhu X., Sun Y., Luo X., Lei H., Wang B., Song W., Yang Z., Dai J., Shi D. and Dou S., *J. Magn. & Magn. Mater.*, **322** (2010) 242.
[31] Houze E. and Nechtschein M., *Phys. Rev. B*, **53** (1996) 14309.
[32] Steigmeier E. F. and Harbeke G., *Phys. Kondens. Mater.*, **12** (1970) 1.
[33] Malicka E., Waskowska A., Skrzypek D., Sitko R. and Kaczorowski D., *J. Solid State Chem.*, **182** (2009) 3149.
[34] Waskowska A., Gerward L., StaunOlsen J., Morgenroth W., Malicka E. and Skrzypek D., *J. Phys.: Condens. Matter*, **20** (2008) 425209.
[35] Luo X., Yang Z. R., Sun Y. P., Zhu X. B., Song W. H. and Dai J. M., *J. Appl. Phys.*, **106** (2009) 113920.